JOURNAL OF APPLIED POLYMER SCIENCE VOL. 19, 2545–2562 (1975)

The Fracture of Epoxy- and Elastomer-Modified Epoxy Polymers in Bulk and as Adhesives

W. D. BASCOM, R. L. COTTINGTON, R. L. JONES, and P. PEYSER,
Surface Chemistry Branch, Naval Research Laboratory, Washington, D.C. 20375

Synopsis

The fracture behavior of a piperidine/bisphenol A diglycidyl ether (A) resin has been determined in bulk and as an adhesive using the linear elastic fracture methods developed by Mostovoy.[1] The effect of adding carboxy-terminated butadiene–acrylonitrile (CTBN) elastomer to resin A was investigated. The opening-mode fracture energy ($\mathcal{G}_{Ic}$) of resin A was 120 to 150 J/m^2, and largely attributable to plastic deformation. Fractographic evidence was obtained for plastic flow at the crack tip during crack initiation. Propagation was unstable due to the rate dependence of the plasticity. There were no significant differences in the bulk and adhesive fracture behavior. Addition of 5–15% CTBN to resin A produced minute elastomer particles which increased $\mathcal{G}_{Ic}$ to ~4000 J/m^2 (at 15%). Further CTBN addition resulted in an elastomer–epoxy blend and a decrease in fracture energy. Fractography again indicated that crack initiation involved plastic deformation but that the elastomer had greatly increased the volume in which the deformation occurred. The adhesive fracture of the elastomer–epoxy was found to be strongly dependent on the crack-tip deformation zone size (r_{yc}) in that $\mathcal{G}_{Ic}$ was a maximum when bond thickness was equal to 2 r_{yc}. At bond thicknesses less than 2 r_{yc}, there was a restraint on the development of the plastic zone resulting in lower $\mathcal{G}_{Ic}$ values.

INTRODUCTION

Industrial bonding of load-bearing structures demands adhesives formulated from high-strength, high-modulus polymers. This need has been met to a large extent by the epoxies, notably those based on bisphenol A diglycidyl ether (DGEBA). However, the unmodified epoxies are relatively brittle materials compared to the metals they are called upon to bond. Consequently, elastomers and other "toughening" agents are added to the base polymer but often with a serious loss in tensile strength, modulus, and heat distortion temperature. This trade-off can be lessened by the use of certain elastomers that react *in situ* during epoxy polymerization to form minute elastomer particles. Dual phase formulations of this type have been in use in adhesive technology for at least a decade.[2] However, they were not described in the open literature until McGarry et al.[3] and later Siebert et al.[4,5] reported on epoxy resin systems containing the carboxy-terminated butadiene–acrylonitrile (CTBN) elastomers. They found that the CTBN formed 2- to 5-μ particles in the epoxy which increased the epoxy fracture energy (toughness) many times and that particle formation involved formation of a copolymer by reactions between the epoxy molecule, the CTBN elastomer, and the catalyst or cross-linking agent.

Despite the established use of dual-phase structural adhesive resins, there does not appear to have been any systematic study of their adhesive fracture behavior. Consequently, the work described in this report was concerned with the adhesive fracture of a CTBN-modified diglycidyl ether bisphenol A (DGEBA) epoxy. Methods for studying the fracture of adhesives, based on linear elastic fracture mechanics, have been developed by Mostovoy and Ripling.[1,6] Their approach was utilized here, and our results for the unmodified epoxy were quite comparable to theirs, but we have found a new regime of behavior in the adhesive fracture of the elastomer–epoxy resins.

EXPERIMENTAL

Materials

The epoxy monomer used in this study was the diglycidyl ether of bisphenol A DGEBA) obtained from the Dow Chemical Co. (DER-332) and had a nominal epoxy equivalent weight of 175 ± 3 (theo. = 170) and a viscosity of about 5000 cps at 25°C. The curing agent was piperidine (99.8% Fisher Scientific Co.). The CTBN (B. F. Goodrich Co.) had a nominal molecular weight (number-average) of 3500. All materials were used as received. The resin was prepared by mixing into the DGEBA (or DGEBA + CTBN) 5 phr (parts per hundred weight of the DGEBA) of piperidine and curing at 120°C for 16 hr. Prior to addition of the piperidine, the epoxy mixtures were outgassed in a rotating flash evaporator for small batches (<200 ml) or in a reaction flask.

The aluminum adherends were cut as tapered double cantilever beams (Fig. 1) from 1.3-cm-thick 5086 aluminum alloy plates. The nominal composition of this alloy is 4.0% Mg, 0.5% Fe, 0.5% Mn, 0.4% Si, and <0.2% of other metals. The first step in surface preparation was to cut the edge to be bonded to a "fine" mill finish (~46 μin. CLA) with a rotary fly-cutter. This operation was facilitated by having the height of the two ends of the specimen the same (Fig. 1) so that the beam sat level on the mill bed. After milling, the beams were rinsed with acetone or methyl ethyl ketone to remove gross contamination and then etched in an acid-chromate solution[7] at 68°C for 15 min. The acid was then rinsed off in a bath of flowing tap water for 10 min. Finally, the beams were allowed to dry in ambient laboratory air for about 1 hr.

Methods

Most quantitative treatments of fracture are based on the Griffith criteria,[8]

$$P_c = \left(\frac{2E\gamma_s}{\pi a}\right)^{1/2} \tag{1}$$

where P_c is the stress at fracture, E is the elastic modulus, γ_s is the "surface energy," and a is the crack length. This equation can be derived from simple atomic force considerations for a remotely loaded, edge-notched specimen and is exact only for ideally brittle, linear elastic fracture. Although few if any materials fail in the ideally linear elastic fashion, eq. (1) is nonetheless formally applicable. Berry showed that P_c is proportional to $1/\sqrt{a}$ for PMMA even though the observed fracture energy was much too large.[9] At-

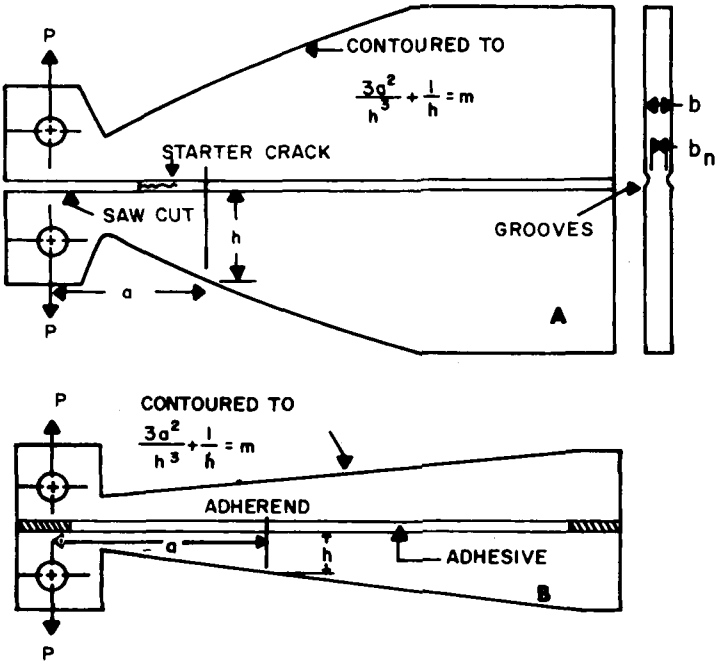

Fig. 1. Tapered-DCB bulk (A) and adhesive (B) test specimens for opening mode fracture.

tempts have been made to account for the high fracture energies but they have not been fully successful, and the resulting expressions are quite complex. Irwin[8] took the approach that the Griffith criteria are formally correct but that the surface energy should be replaced by a strain energy release rate, $\mathcal{G}_c$,

$$P_c = \left(\frac{E\mathcal{G}_c}{\pi a}\right)^{1/2} \tag{2}$$

which includes all the energies involved in fracture, both elastic and inelastic. In the ideally brittle limit, $\mathcal{G}_c = 2\gamma_s$. Valid measurements of $\mathcal{G}_c$ can be made using notched specimens so long as the stress–strain behavior of the specimen *as a whole* is linear elastic which will be the case if the inelastic fracture processes are localized in a relatively small region at the notch tip.

In determining $\mathcal{G}_c$ using double cantilever beams (DCB) the fracture energy is equated to the strain energy at crack initiation. Assuming that the specimen responds elastically (except at the crack tip) then

$$\mathcal{G}_c = 1/2\frac{P_c^2}{2b}\frac{dC}{da} \tag{3}$$

where b is the specimen width and dC/da is the change in the compliance of the specimen with crack length. In the case of a DCB, eq. (3) becomes

$$\mathcal{G}_c = \frac{4P_c^2}{b^2E_b}\left(\frac{3a^2}{h^3}+\frac{1}{h}\right) \tag{4}$$

where h is the beam height and E_b is the bending modulus of the polymer in bulk specimens and the metal in the adhesive specimens. Mostovoy[1] designed a tapered double cantilever beam specimen (Fig. 1) such that dC/da is a constant, m, over the length of the specimen, and eq. (4) becomes

$$\mathcal{G}_c = \frac{4P_c^2}{b^2E_b} m \tag{5}$$

The taper is determined by the bracketed term in eq. (4). The advantages of this specimen is that $\mathcal{G}_c$ is given by the load, P_c, without any need to measure crack length. Also, this specimen design allows the crack to propagate at constant velocity for a constant rate of separation *unless the fracture energy is a function of crack speed.* The DCB specimen, tapered or otherwise, gives the cleavage fracture energy which is only one of three possible modes of fracture, the other two being in-plane shear and torsional shear. Cleavage is generally designated as mode I or opening-mode fracture, and so the corresponding fracture energy is designated as $\mathcal{G}_{Ic}$. The bulk polymer specimens, including the TDCB's, bending modulus bars, and the sheets from which the tensile bars were cut, were all formed by casting the resin into silicone rubber molds (RTV 30, G. E. Silicone products Dept.).

The tapered-DCB specimens for bulk $\mathcal{G}_{Ic}$ determinations were cast with a taper of $m = 3$. They were usually 1.3 cm thick and had square-cut grooves, 0.2–0.3 cm deep and 0.16 cm wide, milled along both sides to guide the crack. This reduction in specimen width is accounted for by modifying eq. (5):

$$\mathcal{G}_{Ic} = \frac{4P_c^2}{bb_nE_b} m$$

where b_n is the plate thickness between the grooves (Fig. 1). A saw cut was made into the specimen, 5 cm from the center of the loading holes. A crack was then started by tapping a knife edge against the end of the saw cut until a short crack formed spontaneously, usually 0.5 to 1.0 cm long. In the case of the epoxy-elastomer specimens it was not possible to induce cracking with a knife edge at room temperature; the most that was achieved was to form a blunt notch. Sharp precracks were formed by cooling the specimen in liquid N_2 before tapping with the knife edge.

The TDCB adhesive specimens were assembled for bonding as shown in Figure 2. The two aluminum halves were held together with spring loaded clamps. Teflon spacers determined the bond thickness. One side of the bond area was sealed with a strip of Teflon coated aluminum foil overlaid with a heat resistant pressure sensitive adhesive tape. The resulting cavity was filled by slowly pouring in the liquid epoxy mixtures. After heat curing the specimen, the tape and foil were stripped away and excess polymer on the beam sides was abraded off. The Teflon-coated foil was used to prevent contamination of the epoxy in the bond with the tape adhesive.

Tensile strengths and moduli were determined using ASTM Method D638-64T (10) and the bending moduli were determined using the four-point loading method.[6] All mechanical tests were performed at 25° ± 3°C on an Instron TT-B a 0.05 in./min (0.13 cm/min) strain rate. The scanning electron microscope was an Advanced Metal Research Model 1000. All micros-

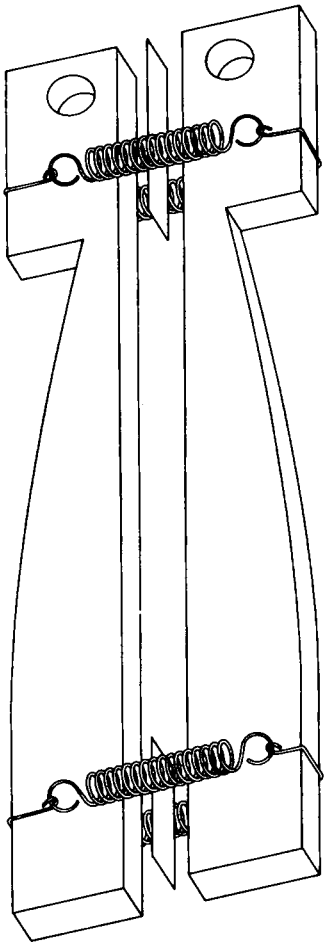

Fig. 2. Expanded view of the tapered-DCB adhesive specimen.

copy specimens were given a coating of gold (~200 Å) by vacuum evaporation prior to SEM examination in order to reduce charging effects. The Perkin-Elmer TMA was used to determine the glass transition temperatures (T_g) and the linear thermal coefficients of expansion ($\alpha_g(l)$).

RESULTS

The fracture energies ($\mathcal{G}_{Ic}$) of the DGEBA–piperidine epoxy polymer are listed in Table I along with the tensile modulus, bending modulus, tensile strength, and glass transition temperature. All of the bulk polymer specimens exhibited unstable crack growth, i.e., whenever a crack initiated it propagated at a faster rate than the cross-head speed (i.e., jumped ahead of the machine) until enough energy was lost to bring the crack to rest. Because of this unstable propagation, the load-displacement curves had a peaked or "saw-tooth" appearance (Fig. 3). The peaks on these curves correspond to crack initiation, $\mathcal{G}_{Ic}^{i}$, and the valleys to crack arrest, $\mathcal{G}_{Ic}^{a}$.

TABLE I
Properties of the DGEBA—Piperidine Epoxy (25°C, 45% RH, 0.13 cm/min)

Tensile yield strength σ_y	727.6 ± 5.7 Kgf/cm²
Tensile modulus E	(3.37 ± 0.05) × 10^4 Kgf/cm²
Bending modulus E_b	3.11 × 10^4 Kgf/cm²
Glass transition temperature	71°C
Fracture energy, bulk	
initiation, $\mathcal{G}_{1c}^{i}$	121 ± 9 J/m²
arrest, $\mathcal{G}_{1c}^{a}$	100 ± 7 J/m²
Fracture energy, adhesive (0.025 cm bond)	
initiation, $\mathcal{G}_{1c}^{i}$	154 ± 29 J/m²
arrest, $\mathcal{G}_{1c}^{a}$	133 ± 21 J/m²

The locus of failure of the adhesive bond specimens was "center-of-bond," as evidenced by the presence of essentially equal amounts of polymer on both fracture surfaces. Like the bulk polymer, they exhibited unstable crack propagation except that the length of unstable cracking was generally shorter, and so the load-displacement curves for the adhesive tests had more peaks.

The regions of crack arrest and initiation were visible on the fracture surfaces as slightly curved lines (fingernail markings) across the width of the specimen. Examination of these regions using SEM revealed a pattern of tear markings (Fig. 4).

The effect of bond thickness on fracture behavior was investigated for the unmodified piperidine–DGEBA system and the results are given in Figure 5. There was a slight increase in $\mathcal{G}_{Ic}^{i}$, but since the standard deviation was as much as 20% for the thicker bond (0.20 cm), the significance of the increase is questionable.

The effects of adding the butadiene–acrylonitrile elastomer to the piperidine-cured epoxy are indicated in Figures 5, 6, and 7. Note the transition in elastomer dispersion from particulate to blend between 15% and 20% CTBN. In the "particulate" region, small inclusions of elastomer 2–5 μ in diameter could be easily observed at 500×. No inclusions were visible in the "blend" material even at 10,000× magnification in the SEM.

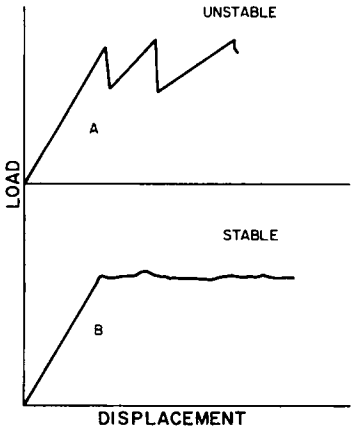

Fig. 3. Load-displacement curves of stable and unstable crack propagation.

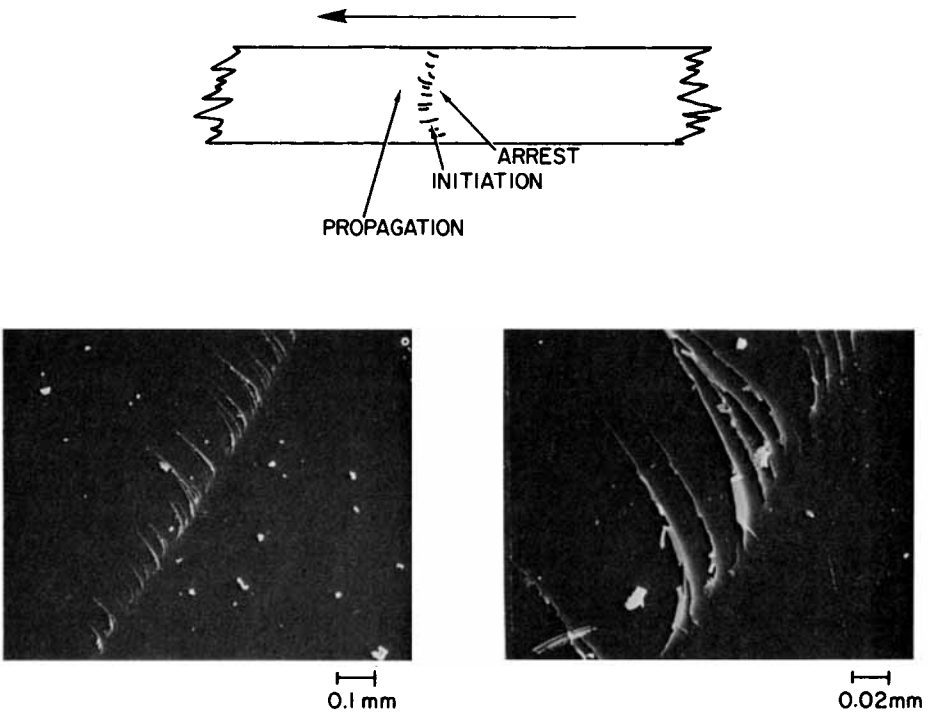

Fig. 4. Markings at an initiation-arrest site on the fractured surface of the piperidine-DGEBA polymer.

In the bulk specimens, the elastomer particles increased the initiation fracture energy by more than 30-fold but had much less of an effect on crack arrest. In fact, the initial cracks usually propagated the entire length of the specimen. At concentrations of 20% and 30%, in the "blend" region, crack propagation was stable and there was a downward trend in the $\mathcal{G}_{Ic}$ values with increasing elastomer concentration.

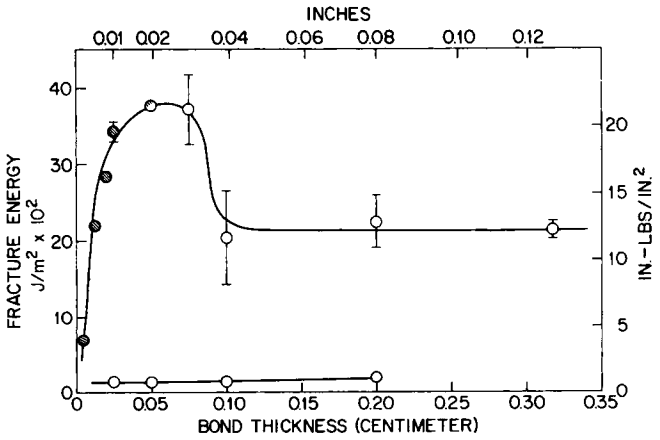

Fig. 5. $\mathcal{G}_{Ic}$ vs. bond thickness. Lower curve is for unmodified piperidine-DGEBA and the upper curve is for 15% CTBN in piperidine-DGEBA. O, unstable propagation; ●, stable propagation.

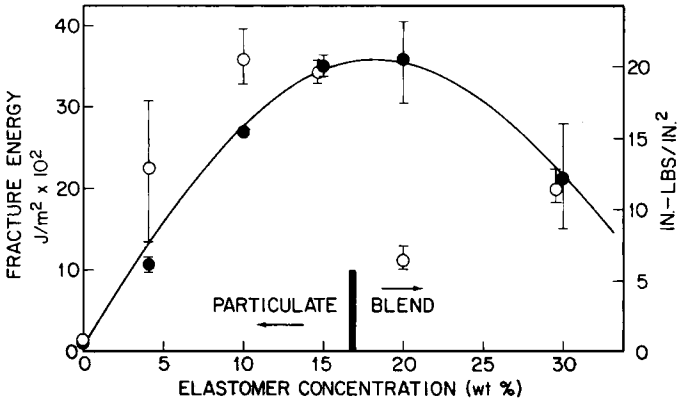

Fig. 6. $\mathcal{G}_{Ic}$ vs. CTBN concentration in piperidine-DGEBA. O, adhesive; ●, bulk.

The adhesive fracture behavior of the elastomer–epoxy compositions was dominated by a strong bond thickness effect. The results for the 15% elastomer resin are presented in Figure 5. Note the maximum in $\mathcal{G}^i_{Ic}$ and the transition from stable to unstable propagation at the maximum.

The effect of bond thickness on the fracture of the CTBN–epoxy in the blend concentration region (30% elastomer) is given in Figure 7. There was a sharp decrease in $\mathcal{G}^i_{Ic}$ with decreasing bond thickness; but, unlike the adhesive fracture of the particulate dispersion resins, there was no maximum and stable propagation was observed at all bond thicknesses.

Although the arrest values of $\mathcal{G}_{Ic}$ could not be obtained from bulk specimens of the elastomer (particle)–epoxy resins it was possible to obtain values from the thick-bond adhesive specimens. Some of these results are listed in Table II, and it is noteworthy that the arrest energies were four times smaller than the initiation energies.

Additional results on the properties of the CTBN–epoxy resins are presented in Figure 11.

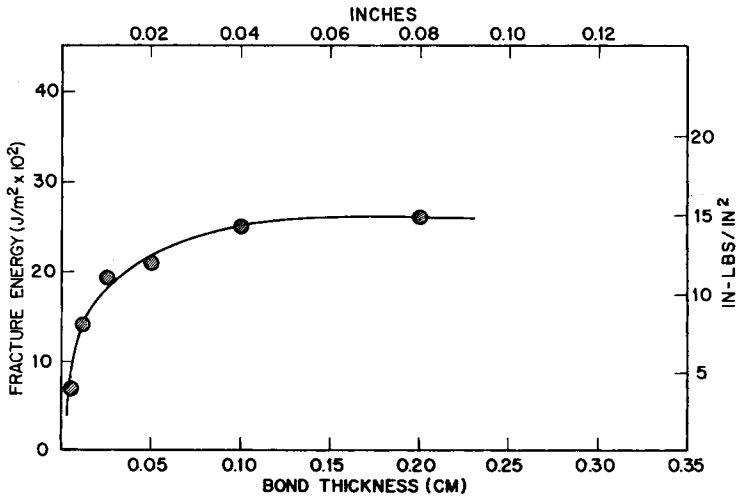

Fig. 7. $\mathcal{G}_{Ic}$ vs. bond thickness. 30% CTBN in piperidine-DGEBA. ●, stable propagation.

TABLE II
A Comparison of Initiation ($\mathcal{G}_{Ic}^{i}$) and Arrest ($\mathcal{G}_{Ic}^{a}$) Adhesive Fracture Energies

CTBN, wt %	$\mathcal{G}_{Ic}^{i}$, J/m²	$\mathcal{G}_{Ic}^{a}$, J/m²	Bond thickness, cm
0	143	121	0.025
4.5	2270	233	0.025
15	2040	457	0.10
15	2250	485	0.20
15	2150	537	0.32

Postfailure examination of the elastomer–epoxy polymers gave some insight into the phenomena involved in the increase in fracture energy and the differences between bulk and adhesive behavior. Thick-bond adhesive specimens which had failed unstably exhibited "fingernail" markings at positions of crack arrest and initiation. There was a distinct whitening of the polymer along these lines. Otherwise the surfaces were relatively featureless. Examination of these markings with the SEM indicated extensive deformation of the elastomer particles and the surrounding matrix. In Figure 8, the stress-whitened region is evident at 100× as a light band perpendicular to the cracking direction. At 200×, this band was found to be comprised of minute,

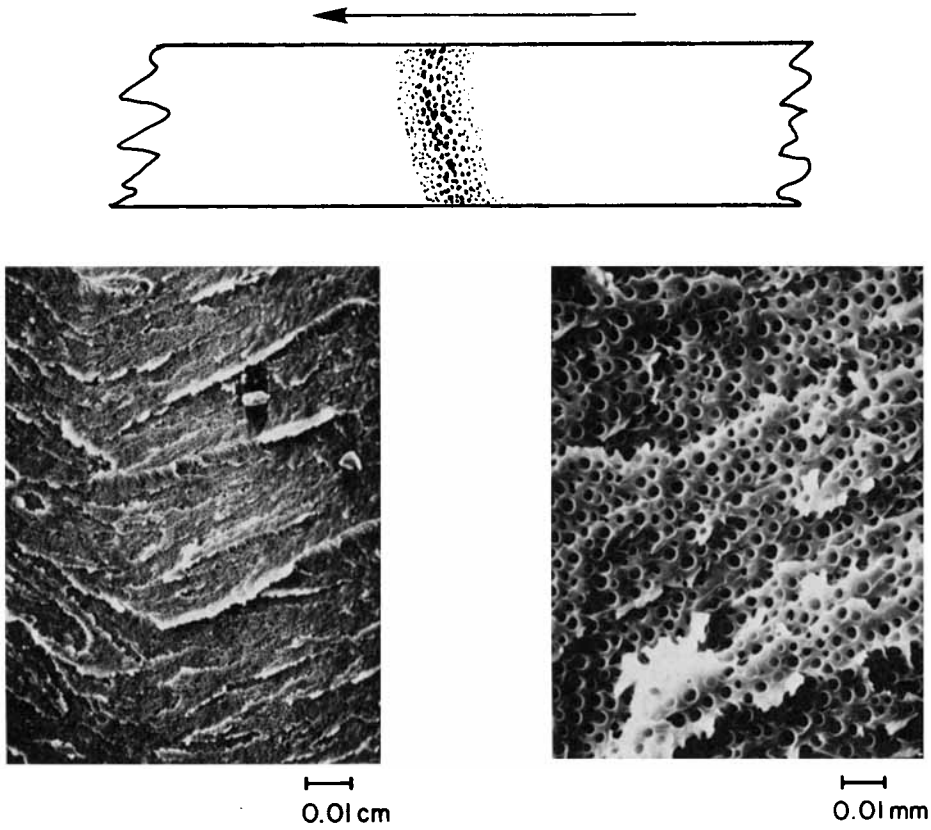

Fig. 8. Markings at an initiation-arrest site on the 15% CTBN-piperidine-DGEBA fracture surface (bond thickness = 0.10 cm).

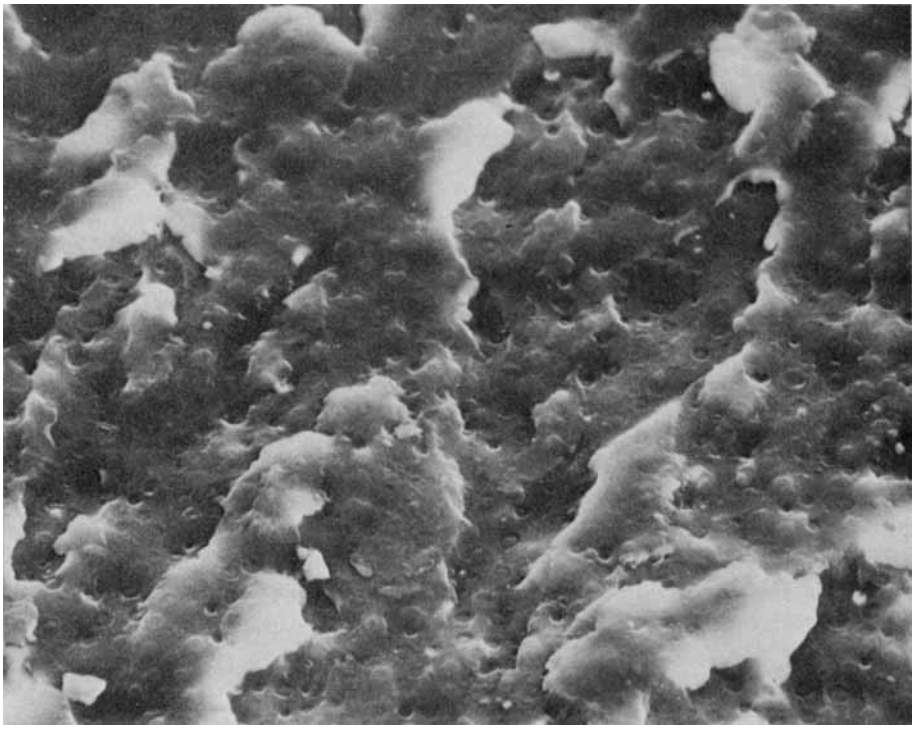

Fig. 9. Appearance of the fast cracking region on the 15% CTBN-piperidine-DGEBA surface.

closely spaced holes in the matrix. Increasing the magnification to 1000× reveals the holes to be well developed in the center of the band. Some of the holes appear to be empty, whereas others are filled. At an area well removed from the stress whitening and where the crack had propagated rapidly (Fig. 9), there was very little evidence of hole formation although the elastomer particles were clearly evident.

The thinner adhesive bonds (0.05 to 0.013 cm) of the 15% CTBN–epoxy suffered complete stress whitening when fractured. The entire polymer layer which initially had been a dark brown had been turned to a very light tan. Failure had left islands of this whitened polymer on both surfaces. Examination of these features with the SEM revealed massive deformation that produced material having the appearance of Swiss cheese (Fig. 10). The holes generally had a spherical shape except near the base of the islands. The larger of these holes seem to be empty. Part of the failure process involved a peeling of the material into thin sheets. Note also the "floor" around the islands. Casual observation might suggest that failure had occurred at the metal/polymer interface, but close examination reveals evidence of polymer and particles of the elastomer in this floor. Evidently, failure was in the adhesive although close enough to the interface to cause replication of the machine markings on the metal.

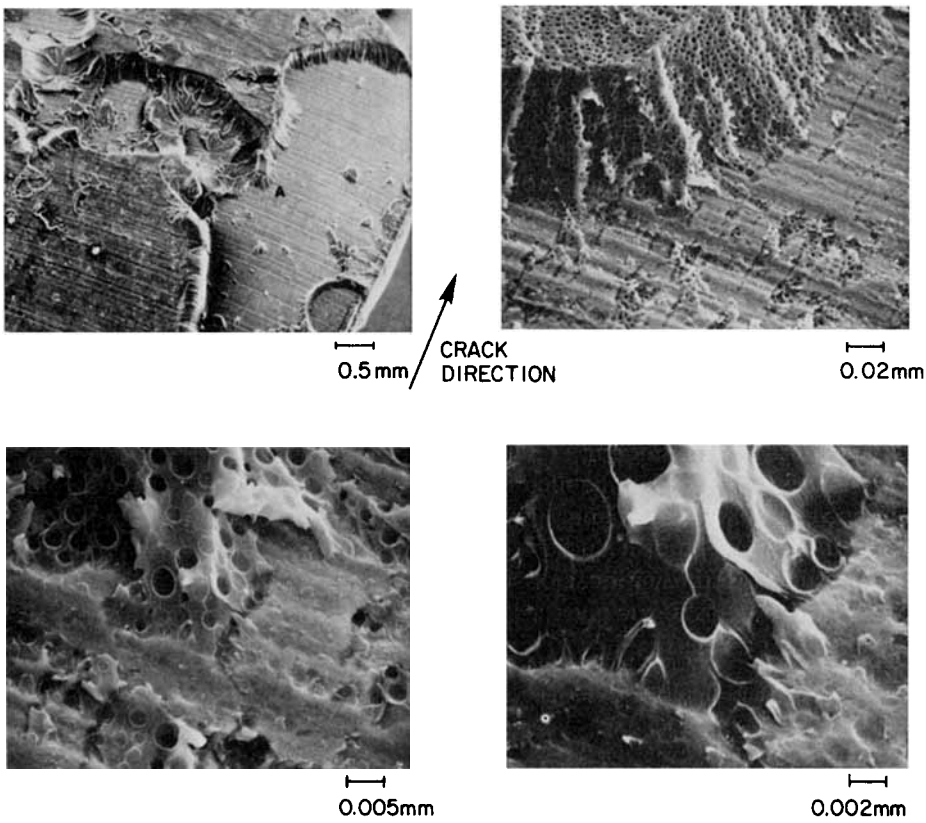

Fig. 10. Evidence of the complete deformation of the adhesive layer in a 0.025 cm bond of the 15% CTBN-piperidine-DGEBA polymer.

DISCUSSION

Unmodified Epoxy

The fracture energies of the piperidine–DGEBA epoxy (Table I) were in the same range of 100 to 1000 J/m^2 that have been reported for other epoxies[1,6] and for polyesters.[11] These values are much larger than even the most generous theoretical estimate for purely brittle fracture. Following the arguments of Berry,[9] the most that can be attributed to molecular cleavage is 0.5 J/m^2 assuming that carbon–carbon bonds are being broken and that the polymer chains were oriented perpendicular to the direction of crack propagation and were as closely packed as possible. It is generally agreed that these high energies are due to inelastic deformation processes at the crack tip.

The evidence of plastic flow along the line of crack initiation in Figure 4 is certainly a strong indication that deformation was a major factor in the fracture of the epoxy. The deformation appears to be highly localized in that the tearing originated from separate, randomly distributed points along the crack front. Similar fractographic evidence of localized plastic flow during crack initiation has been reported for unmodified epoxies by Patrick[12] and for phenolics by Nelson and Turner.[13]

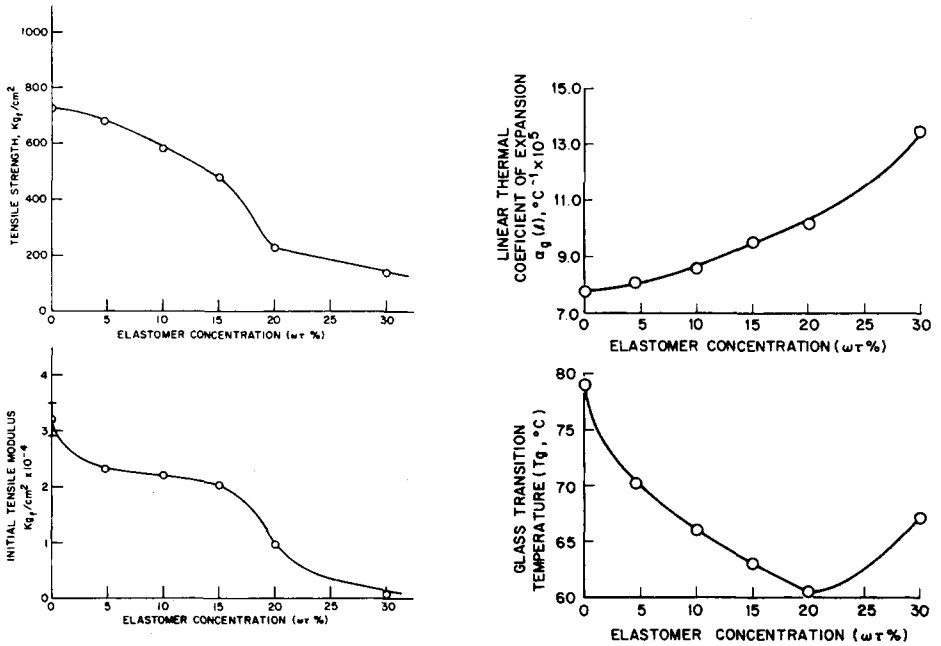

Fig. 11. Effect of CTBN concentration in piperidine–DGEBA on tensile strength, modulus, glass transition temperature, and linear thermal coefficient of expansion.

Once crack propagation was initiated, the degree of plastic deformation declined to an imperceptible level so that in Figure 4 the fingernail marking was followed by an essentially featureless fracture surface. This, of course, is the essence of the strain rate sensitivity of glassy polymers. An initiated crack propagates spontaneously because the speed exceeds the relaxation time for plastic flow and $\mathcal{G}_{Ic}$ decreases with increasing crack speed.

Arrest occurs in these tapered DCB specimens when (and if) the beams lose sufficient kinetic energy (by unbending) that the remaining stored energy becomes equal to the "$\mathcal{G}_I$" of the material ahead of the moving crack. However, it is problematical as to whether the arrest energy is a material characteristic. Unlike the initiation energy, which is defined at a critical condition, eq. (3), the arrest energy is associated with a crack propagating at an unknown rate. Nonetheless, $\mathcal{G}^a_{Ic}$ values were found here to be as reproducible as the initiation energies (see Tables I and II), and this was also the case in the work of Mostovoy and Ripling.[1,6]

Elastomer-Modified Epoxy

The CTBN elastomers are soluble in the liquid amine–epoxy resins but react to form an elastomer–epoxy copolymer which precipitate out early in the heat cure to form 2- to 5-μm particles.[3,4] These elastomer particles increase the resin fracture energy by at least a factor of ten as shown by McGarry.[3] In the work reported here, the initiation fracture energy $\mathcal{G}^i_{Ic}$ of the piperidine–DGEBA resin was increased over the unmodified resin by a factor of 30 to 40. However, there was not a comparable increase in the arrest energy $\mathcal{G}^a_{Ic}$. In fact, the energy input for crack initiation in the bulk specimens was

so great that the rate of energy loss was too slow to prevent the crack from propagating the length of the beam thereby prohibiting any determination of arrest energies. Adhesive arrest energies for two of the CTBN (particle)–epoxy compositions (5% and 15% CTBN) were obtained from the thick-bond adhesive specimens (Table II). Evidently, the rate of strain energy loss from the stiff adhesive specimens was rapid enough to allow crack arrest, whereas this was not the case for the bulk specimens.

Crack initiation in the bulk (and thick-bond) specimens of the CTBN (particle)–epoxy involved massive plastic deformation resulting in a broader fingernail marking than on the unmodified epoxy (compare Figs. 4 and 8). Within the marking there was an obvious distortion of the elastomer particles. Indeed, the deformation had been sufficient to rupture the particle material and leave the resulting hole empty (or possibly lined with the elastomer), although occasionally a small sphere of elastomer could be seen within a hole. The nearly spherical shape of the holes in Figure 8 indicates that the elastomer particles were deformed by an essentially triaxial dilatation. This is consistent with the triaxial stress distribution expected at the crack root in these specimens which fail in plane strain.

Once initiated, the crack propagated rapidly and spontaneously just like the unmodified resin. In the region of fast cracking, illustrated in Figure 9, the strain rate was too high to allow significant plastic flow. Indeed, the elastomer particles show little evidence of deformation. However, the large amount of strain energy available to the moving crack did produce crack branching which left the fracture surface very rough.

Discussion of the effect of bond thickness on $\mathcal{G}_{Ic}$ and the fracture behavior of the thin-bond adhesive specimens is deferred to the next section.

The behavior of CTBN–epoxy blend compositions (20% and 30% CTBN) was dramatically different from that of the elastomer particle dispersions. Generally speaking, the blends exhibited a rubber-like behavior by failing in a tearing fashion in contrast to the brittle-like fracture of the particulate dispersions. The blends gave stable crack propagation in bulk and at all bond thicknesses, and the fracture surfaces had a very rough appearance.

Micromechanics of Failure

It is instructive to consider the fracture behavior of these polymers from the viewpoint of an elastic-plastic material.[13] (Deformation is elastic up to the yield stress σ_y and then becomes fully plastic.) A schematic of the zone at a crack tip according to this model is shown in Figure 12. There is a small

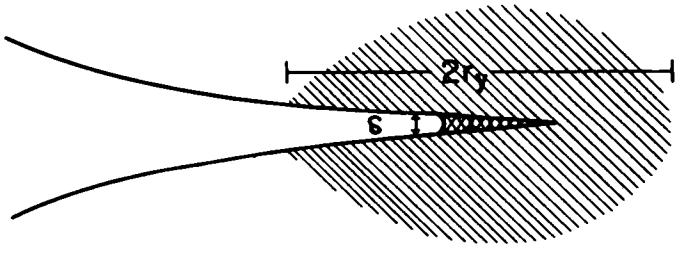

Fig. 12. Schematic drawing of the crack opening displacement model of an elastic-plastic material.

TABLE III
Plastic Zone Diameter

CTBN, wt%	$2r_{yc}$, cm: Eq. (7)	$2r_{yc}$, cm: Exp. estimate	Propagation in a 0.025-cm bond
0	0.00082	0.0004	unstable
4.5	0.0124		unstable
10	0.021		stable
15	0.035	0.015	stable
20	0.070		stable
30	0.022		stable

slice of plastically deformed material that is at failure strain, ϵ_f ($\epsilon_f \gg \epsilon_y$) with a larger zone of radius r_y in which the stress is σ_y and the strain is ϵ_y, the yield strain. Furthermore, the crack root is not sharp but has a characteristic dimension δ_I, the crack opening displacement. At the critical value of δ_I, the fracture energy is given by

$$\mathcal{G}_{Ic} = \delta_{Ic}\sigma_y \tag{6}$$

The radius of the plastic zone is given by

$$r_{yc} \approx \frac{1}{6\pi}\frac{E}{\sigma_y^2}\mathcal{G}_{Ic} \tag{7}$$

for plane strain conditions at the crack tip (i.e., no lateral contraction). Values of $2r_{yc}$ were calculated from the experimental data and are listed in Table III. Clearly, the elastomer addition had a major effect in increasing the critical deformation zone size.

This was confirmed by measurements of the markings on the fracture surfaces of the unmodified and 15% CTBN–epoxy specimens. The $2r_y$ value of the former was estimated as the width of the base from which the tear markings emanate in Figure 4. The value for the 15% CTBN–epoxy was taken as one half the width of the stress whitened zone in Figure 8. In making these estimates, it was assumed that only part of the fracture marking occurs at initiation and that the remainder occurs in the early stages of propagation.

The importance of r_y in determining $\mathcal{G}_{Ic}$ can be seen by rearranging eq. (7) and introducing the yield strain ($\epsilon_y = \sigma_y/E$),

$$\mathcal{G}_{Ic} \approx 6\pi\sigma_y\epsilon_y r_{yc} \tag{8}$$

The yield stress actually decreases with the addition of CTBN (Fig. 11). Furthermore, the elastomer has little effect on yield strain (see Appendix). Therefore, the principal effect of the elastomer (particulate or blend) on fracture is to allow the energy to be dissipated into a relatively large volume of material at the crack tip. Part of this plasticity of the elastomer (particle)–epoxy may be due to a small concentration of molecularly dispersed elastomer undoubtedly present along with the particles. The relatively sharp drop in tensile modulus at 4.5% CTBN compared to a more gradual decline up to the blend compositions may reflect this "equilibrium" concentration. A second, equally important, factor is that because the particles form by essentially a precipitation process,[4,5] it is reasonable that the boundary between parti-

cle and matrix is diffuse and thus a highly plasticized region which inhibits microcrack initiation and propagation. As a result of these two effects, a large plastic zone develops at the crack tip before local microcracks can coalesce and advance the main crack front. This mechanism of polymer toughening by dispersed elastomer particles has been discussed by Buchnall[14] for PMMA and by McGarry[15] for CTBN–epoxy resins.

The same considerations of eq. (8) can be made for the CTBN (blend)–epoxy compositions. However, the molecular behavior at the crack tip would be quite different. The development of the plastic zone in the blend materials probably involves distortion and alignment of long polymer chains (e.g., the homogeneously dispersed CTBN–epoxy adduct[5]).

Referring now to the effect of bond thickness on $\mathcal{G}_{Ic}$ (Fig. 5), the maximum in fracture energy and the transition from stable to unstable propagation occurred when the bond thickness and the plastic zone diameter were about equal. The transition occurred between bond thicknesses of 0.025 and 0.050 cm and the plastic zone size of the 15% CTBN–epoxy was 0.035 cm. Further evidence for the importance of the zone size relative to the bond thickness is found in the fracture behavior of the other elastomer-epoxy compositions, i.e., 4.5%, 10%, 20%, and 30% CTBN. They were all tested in specimens having bond thicknesses of 0.025 cm and they all had plastic zone sizes greater than 0.025 cm except for the 4.5% CTBN material (Table III). The $2r_{yc}$ value for the latter was only 0.0125 cm, and accordingly all of these compositions, except the 4.5% CTBN, exhibited stable propagation.

The reasons for the maximum in $\mathcal{G}_{Ic}^{i}$ with bond thickness are not entirely obvious. The decrease in toughness as the thickness was reduced to less than the inherent deformation zone size of the resin is easily seen as a restraint on the resin plasticity. However, the reason for the rise in $\mathcal{G}_{Ic}^{i}$ in the approach to the maximum as the bond thickness is reduced toward $2r_{yc}$ is not clear and, as outlined below, may be related to deviations from plain-strain conditions. We consider these two effects separately starting with the decrease in toughness for bond thicknesses less than the zone diameter.

Reduction in bond thickness after the maximum in $\mathcal{G}_{Ic}$ was accompanied by a change in failure mode in that crack propagation ceased to be a center-of-bond cleavage. As indicated in Figure 13, a whitened zone extending the thickness of the adhesive layer moved down the bond as the specimens failed with the most intense whitening at the boundaries. Actual separation was not observed for several millimeters behind this band. Postfailure examination found the entire layer stress whitened and separation had occurred near both of the adhesive/adherend interfaces (Fig. 10). It would appear that fail-

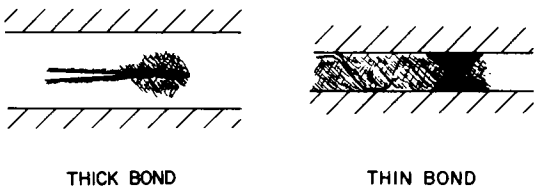

Fig. 13. Schematic of stress-whitened zone in thin ($<2r_{yc}$) and thick ($>2r_{yc}$) bond adhesive specimens of 15% CTBN–epoxy resin.

ure had occurred by a "boundary shear" due to the high differential shear stress that develops where the plastic zone intersects the metal/polymer boundary. The thinner the bond, the smaller the volume of resin available to accommodate strain energy by deformation. This region of decreasing $\mathcal{G}_{Ic}$ with bond thickness might be viewed as a region of *plastic restraint*. Note, however, that the effect cannot be rigorously thought of as a reduction in $2r_{yc}$ since eq. (8) expresses a critical condition for cleavage fracture. Shear failure near the interface occurred before the critical value of $2r_y$ was attained. An extreme example of plasticity restraint is provided by the 20% CTBN–epoxy composition. The adhesive fracture energy of this material was 1100 J/m^2 at a bond thickness of 0.025 cm, less than one third the bulk value (Fig. 6). This difference is not surprising considering that the plastic zone size (0.07 cm, Table III) was nearly three times the bond thickness.

In the region of boundary shear failure, crack propagation was stable which implies that the shear rate did not exceed the relaxation times of the deformation involved. Also, there was a transition point—the half-shaded point at the maximum in Figure 5—where cracking first developed by boundary shear but then a point of instability was reached and the crack jumped forward. This would appear to be a marginal situation where small variations in bond thickness and resin composition cause the fracture conditions to waver between unstable cleavage and stable boundary shear.

The adhesive $\mathcal{G}^i_{Ic}$ values in the thick ($>2r_{yc}$) bond region were anomalous in several respects. First of all, the results for the 15% elastomer (particles)–epoxy rose abruptly as the bond thickness was reduced to give the maximum characteristic of the data in Figure 5. It is interesting that the adhesive toughness values at these bond thicknesses are also lower than the $\mathcal{G}^i_{Ic}$ of the bulk resin. In addition, there was considerable scatter in these data. As for the rubbery 30% elastomer (blend)–epoxy the data did not show a maximum, extrapolated to the bulk toughness value and the data scatter was considerably less than for the 15% elastomer–epoxy resin.

The differences in the adhesive fracture of these two resin compositions may be a reflection of their different modes of failure. The 15% composition of elastomer particles in an epoxy matrix behaved like an elastic-plastic material by exhibiting a distinct plastic zone, whereas the 30% elastomer–epoxy blend failed by a tearing action much like any rubber. Strict application of eqs. (3) *et seq.* involves two assumptions: (a) plain-strain conditions and (b) restraint of the resin by the high-modulus adherends to such a degree that the adhesive layer can be ignored in the stress analysis. Both conditions are met for the relatively stiff, unmodified epoxy resin in thin (<0.05 cm) bonds,[16,17] but may not be valid in thick bonds of the 15% composition or at any bond thickness of the rubbery 30% composition (including the bulk material). Deviations from these assumptions, i.e., toward a plane-stress condition or lower elastic restraint by the adherends would tend to give errantly low calculations of $\mathcal{G}^i_{Ic}$.

Regardless of the uncertainties in interpreting the thick bond data, it is clear that optimum adhesive fracture toughness, and adhesive strength, occur when the bond thickness is close to the deformation zone size of the adhesive resin. Actually, since stable propagation is clearly advantageous, the optimum thickness would be slightly less than $2r_{yc}$.

TABLE IV

CTBN, wt-%	σ_y/E	Eq. (9)
0	0.022	0.061
4.5	0.026	0.062
10	0.024	0.059
15	0.023	0.059
20	0.025	0.062
30	0.074	0.131

SUMMARY

Crack initiation of the unmodified epoxy was characterized by highly localized plastic deformation which accounts for measured fracture energies 100 to 1000 times the theoretical brittle fracture energy. Propagation was generally unstable due to the rate sensitivity of the polymer. Adhesive and bulk fracture energies were essentially identical.

The *in situ* formation of CTBN elastomer particles in the piperidine–DGEBA epoxy increased the fracture energy by a factor of 30 to 40. Crack propagation was still unstable with arrest energies of only four times the unmodified epoxy. The principal effect of the elastomer particles was to increase the plastic zone from about 0.001 cm to as much as 0.035 cm. This appears to be due to a highly flexibilized boundary between the epoxy matrix and the elastomer particles, preventing microcrack formation. The adhesive fracture of the elastomer–particle epoxy exhibited a strong dependence on bond thickness. There was a maximum in fracture energy when the bond thickness was approximately equal to the plastic zone size. The reduction in toughness as the bond thickness was reduced below this maximum was caused by a restraint in the development of the plastic deformation zone. This lowered the fracture energy and also caused a transition from unstable to stable propagation. Anomalous behavior of the "thick bond" specimens may be an artifact attributable to deviations in the assumptions made in calculating fracture energy.

At CTBN concentrations of more than 15% an elastomer–epoxy blend was formed. This change in the elastomer distribution resulted in lower adhesive and bulk $\mathcal{G}_{Ic}$ values and all exhibited stable crack propagation. There was a decrease in adhesive $\mathcal{G}_{Ic}$ for bonds thinner than 0.05 cm but no maximum with bond thickness.

APPENDIX

Effect of CTBN on Yield Strain

DiBenedetto and Trachte[19] consider that the microstrain in polymers is composed of an elastic component, σ_y/E, and a "viscous" strain that can be estimated from the change in free volume. They give an expression for the yield strain,

$$\epsilon_y = \frac{\sigma_y}{E} + \left(\alpha_g - \alpha_{gc}\frac{v_e}{v}\right)\left(\frac{\Delta T_g}{1-2\nu}\right) \quad (9)$$

where α_g and α_{gc} are the volumetric thermal coefficients of expansion [$\alpha_g = 3\alpha_g(l)$] for the polymer at temperature T and for the polymer in a "close-packed" condition; v and v_e are the corresponding specific volumes; $\Delta T_g = (T_g - T)$; and ν is Poisson's ratio (ca. 0.35). The close-packed

condition would correspond to an idealized equilibrium glass. Unfortunately, no values of α_{gc} are available, and so for present purposes it is ignored. This will tend to overestimate the absolute value of the yield strain but should not invalidate comparisons of ϵ_y for different compositions.

The effect of CTBN addition to the piperidine–epoxy on the yield strain is presented in Table IV. Clearly, there was little change in ϵ_y up to 30% CTBN, at which point the elastomer imparts a distinctly "rubbery" character to the epoxy. The data used in eq. (9) to calculate ϵ_y are given in Figure 11.

The authors wish to thank Dr. S. Mostovoy, Materials Research Laboratory, Chicago, and Prof. H. T. Corten, University of Illinois, for their comments during the course of this study. They are also very grateful to Mr. Charles Henderson and Mr. Jack L. Bitner of this Laboratory for their most helpful advice in the experimental aspects of the work. Financial support for this research was provided, in part, by the Naval Materials Command.

References

1. S. Mostovoy and E. J. Ripling, *J. Appl. Polym. Sci.*, **10**, 1351 (1966).
2. J. C. Bolger, in *Treatise on Adhesion and Adhesives*, Vol. 3, R. L. Patrick, Ed., Dekker, New York, 1973, p. 1.
3. J. N. Sultan, R. C. Laible, and F. J. McGarry, *Appl. Polym. Symp.*, **6**, 127 (1971).
4. E. H. Rowe, A. R. Siebert, and R. S. Drake, *Mod. Plast.*, **47**, 110 (1970).
5. A. R. Siebert and C. K. Riew, *Amer. Chem. Soc. Prepr., Organic Coatings Div.*, **31**, 555 (1971).
6. S. Mostovoy and E. J. Ripling, *J. Appl. Polym. Sci.*, **15**, 641 (1971).
7. N. J. DeLollis, *Adhesives for Metals*, Ind. Press, 1970, p. 29.
8. A. S. Tetelman and A. J. McEvily, *Fracture of Structural Materials*, Wiley, New York, 1967, p. 51.
9. J. P. Berry, in *Fracture Processes in Polymeric Solids*, Rosen, Ed., Interscience, New York, 1964, p. 157.
10. *Book of ASTM Standards*, Part 27, Plastics, ASTM, Philadelphia, 1967, p. 190.
11. L. J. Broutman and S. Sahu, *Mater. Sci. Eng.*, **8**, 98 (1971).
12. R. L. Patrick, in *Treatise on Adhesion and Adhesives*, Vol. 3, R. L. Patrick, Ed., Dekker, New York, 1973, p. 163.
13. B. E. Nelson and D. T. Turner, *J. Poly. Sci., Poly. Phys. Ed.*, **10**, 2461 (1972).
13. J. R. Rice, in *Fracture, An Advanced Treatise*, Vol. II, Liebowitz, Ed., Academic Press, New York, 1968, p. 191.
14. C. B. Bucknall and R. R. Smith, *Polymer*, **6**, 437 (1965).
15. J. N. Sultan and F. J. McGarry, *Polym. Eng. Sci.*, **13**, 29 (1973).
19. A. T. DiBenedetto and K. L. Trachte, *J. Appl. Polym. Sci.*, **14**, 2249 (1970).

Received July 16, 1974
Revised January 29, 1975